Analysis of the performance of a Transverse Flux Permanent Magnet (TFPM) wind generator with passive compensated diode-bridge rectifier considering saturation

Mehdi Taghizadeh Kakhki
Laboratoire d'Électrotechnique, d'Électronique de Puissance et de Commande Industrielle (LEEPCI), Université Laval
Québec, QC, CANADA
mehdi.taghizadeh.1@ulaval.ca

Maxime R. Dubois
Department of Electrical and Computer Engineering
Université Laval
Québec, QC, CANADA
mrdubois@gel.ulaval.ca

Abstract – This paper examines the feasibility of employing passive compensation as the simplest way to overcome the limitations of an uncontrolled rectifier for a TFPM generator in the context of a wind energy conversion system. Simulation models are used to compare the series and shunt compensation considering saturation effect. The results indicate the potential of the shunt compensated diode rectifier as an efficient and inexpensive rectifier for a TFPM machine.

I. INTRODUCTION

Due to their high torque density, transverse flux permanent magnet machines are good candidates as wind turbine generators [1]. An uncontrolled bridge rectifier could not be used with a transverse flux machine due to its high stator reactance [2]. The objective of this study is to examine the possibility of using an uncontrolled bridge-rectifier with passive compensation for variable speed transverse flux machines. Both shunt compensated and series compensated Voltage Source Rectifiers (VSRs) will be analyzed.

Since the analytical method will be very complicated in the presence of saturation and in discontinuous conduction mode, simulation will be used to analyze the variable speed machine-rectifier combination.

I. SHUNT COMPENSATED VSR CONSIDERING SATURATION

In order to compensate the source reactance, a shunt capacitor might be used with the plain diode rectifier as shown in figure 1, where the TFPM machine is represented by the sinusoidal source (E_g) in series with the saturable inductance (L_g) and the source resistance (R_g).

Simulation is used to find the operating conditions for which maximum power could be extracted from the source at nominal frequency for the circuit of figure 1. The values chosen for the circuit parameters are shown in Table I. The current –flux characteristic used for the saturable inductance model is shown in figure 2.

$E_{g,n}$ and I_n are used as base values for voltage and current respectively. The base values for power (P_{base}) and for the compensation capacitor (C_{base}) are chosen as follows:

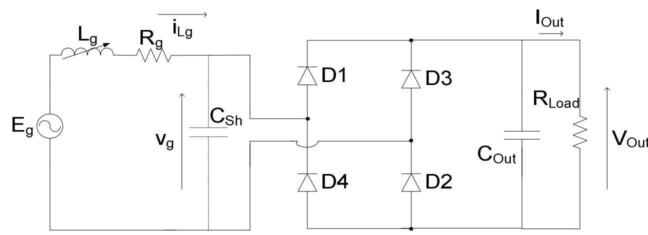

Fig. 1: Shunt compensated diode-bridge rectifier with constant voltage load.

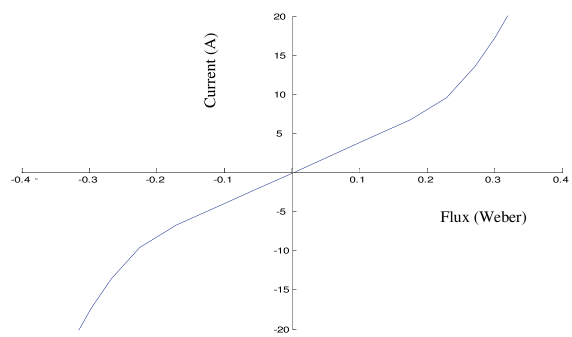

Fig. 2: The Current-Flux characteristic of the saturable inductance model.

TABLE I
Circuit parameters and their respective values

Rated Ideal source voltage $E_{g,n}$	60Vrms
Rated source current I_n	15 A
Frequency f_n	50 Hz
Unsaturated reactance $X_{g,unsat}$	8.168 Ω (2.04 pu)
Saturated reactance $X_{g,\ sat}$	2.51 Ω (0.627 pu)
Source resistance R_g	R_g=0.4 Ω (0.1 pu)
Base value for the capacitor C_{base}	389.7 µF
Output capacitor C_{Out}	25.7 pu

$$P_{base} = (E_g I_n - R_g\ I_n^2)$$
$$C_{base} = (2\pi f_n)/L_g$$

For the purpose of analysis, the displacement factor ($\cos(\varphi)$) will be defined as that of the source E_g, i.e.:

$$DPF = \cos(\varphi) = \frac{P_g}{E_g I_{L_g,1(rms)}} ,$$

and distortion factor (DISF) will be defined as:

$$DISF = \frac{I_{L_g,1(rms)}}{I_{L_g(rms)}} ,$$

where P_g is the active power extracted from the source E_g and $I_{Lg,1(rms)}$ is the fundamental component of the source current.

The shunt capacitor (C_{Sh}) is varied from 0.1 to 1.2 pu with 0.1 pu steps and load resistance is varied between 0.5 to 7 pu with 0.5 pu steps. The results for output power are shown in figure 3. The results included are only those for which the RMS value of the source current does not exceed I_n=2I_{sc}, where I_{sc} is the short circuit current.

It should be noted that the peak power value will be an approximation whose precision depends on the step size chosen for the C_{Sh} and R_{Load}. Repeating the simulation with a higher resolution shows that for source currents smaller or equal to I_n, a capacitor value equal to 0.625 pu will give the highest output power. Figure 4 (b) shows the source current waveform for nominal conditions at which maximum power could be extracted from the source.

To find out the output power in applications with variable EMF voltage and frequency (as in the case of a variable speed wind generator), the capacitor was chosen to be 0.625 pu and the EMF voltage and frequency were varied simultaneously between 0.3 and 1.4 pu. Load resistance varied between 0.5 to 7 pu. The results for output power are partially shown in figure 5. As before, the results included are only those for which the RMS value of the source current does not exceed I_n=2I_{SC}.

As expected, the 1 pu source EMF and frequency will give the highest power and the peak power will shift to lower values of R_{Load} as E_g decreases. DPF (cos(φ)) and distortion factor for peak power condition at each source frequency (source EMF) are shown in figure 6. It is interesting to see that distortion will be small during the whole range, though it will be considerably lower (DISF close to unity) at low

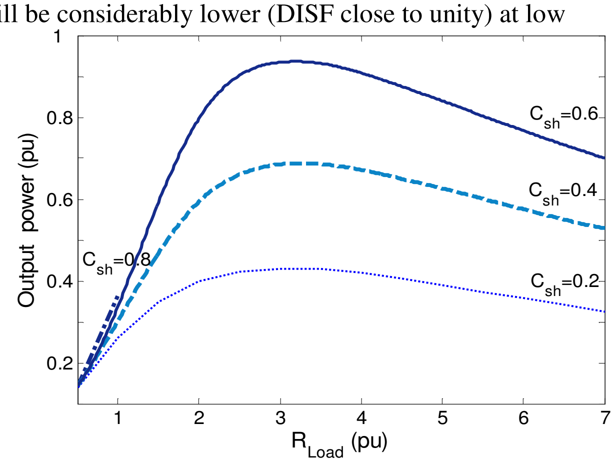

Fig. 3: 2D representation of the simulation results for the shunt compensated VSR at nominal frequency, X_g=2.04 pu @50Hz.

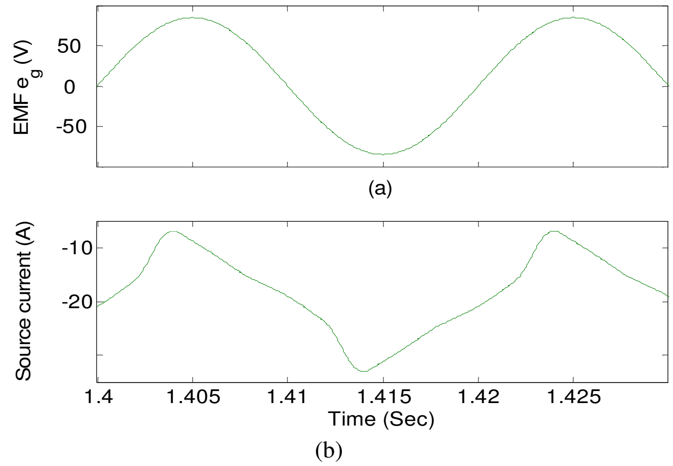

Fig. 4: (a) The source EMF voltage, (b) source current for the saturable inductor with C_{Sh}=0.6 pu, E_g=1 pu, f=1 pu.

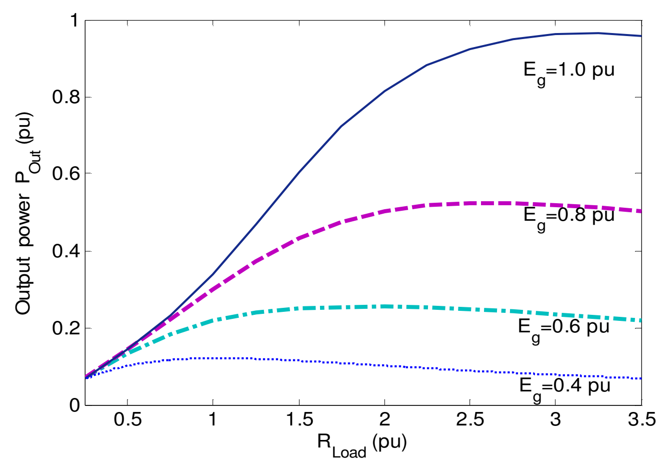

Fig. 5: Simulation results for the shunt compensated VSR, C_{Sh}=0.625 pu with variable EMF voltage-frequency.

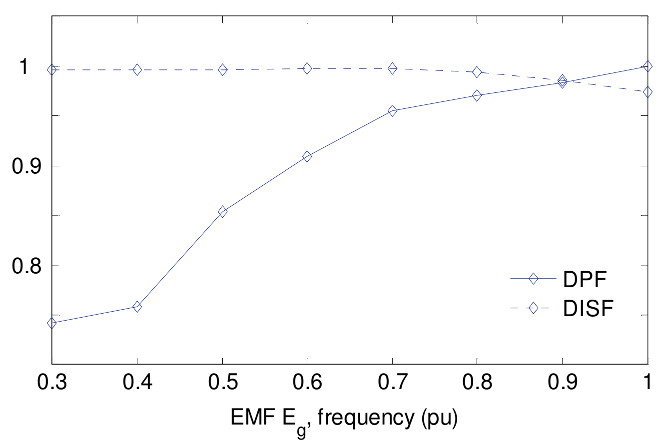

Fig. 6: cos(φ) (DPF) and distortion factor (DISF) characteristics versus source frequency (EMF voltage) for shunt compensated VSR with saturable source inductance.

speeds due to the fact that load current will be lower (saturation has a less pronounced effect) and the rectifier will still remain in the continuous conduction mode. The displacement factor, on the contrary, will decrease at low speeds, as expected, due to overcompensation which means increased reactive power generation at low speeds. The peak extractable power at each speed (frequency-EMF voltage) is presented in figure 7.

The available power from the wind turbine can be expressed as [3]:

$$P_{Turbine} = \frac{1}{2}\rho C_p A v^3 , \qquad (1)$$

where ρ is air density, υ is the wind speed, A is the rotor swept area, and C_p is power coefficient.

Tip speed ratio is a physical characteristic of the wind turbine and is defined as λ= ωR/υ, where R is the radius of the turbine, and ω is the turbine angular velocity in rad/sec.

C_P is assumed to be constant so that maximum power could be extracted from the turbine. This means that λ will also be constant and we have:

$$\omega \propto v ,$$

and

$$P_{Turbine} \propto v^3 \propto f^3$$

The second curve of figure 7 (dotted) shows the optimal turbine power ($P_{Turbine}$) curve. It is assumed that the turbine is dimensioned so that at nominal speed, $P_{Turbine}$ is equal to maximum extractable output power.

Comparing the two curves it could be seen that the peak extractable output power, at each turbine speed, will be always greater than the turbine optimal power.

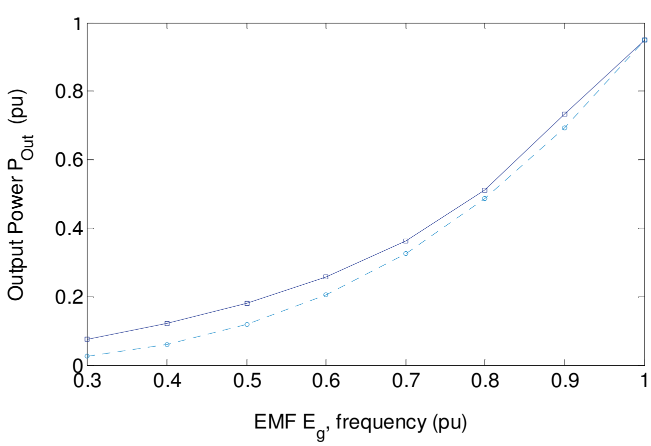

Fig. 7: Maximum extractable output power versus source frequency for C_{Sh}=0.625 and a frequency proportional to wind speed (line), the optimal turbine power curve (dotted).

This will not be the case for applications other than wind turbines where such restriction does not exist for the available source power.

II. SERIES CAPACITOR COMPENSATION CONSIDERING SATURATION

As a second option, we may compensate the large stator reactance by a series capacitor. To see the effects of series compensation, similar to the shunt compensation case, simulation was used to find the operating conditions at which maximum power could be extracted with series compensated rectifier of figure 8. The circuit parameters are similar to the previous case. Again, the simulation with a variable speed (frequency-EMF voltage) and variable load was used to find the peak power at each frequency. Examining the source current waveform for peak power at various speeds shows that, while the rectifier will be in continuous conduction mode at nominal conditions (figure 9(b)), at 0.3 pu speed, it will operate in discontinuous conduction mode as shown in figure 10 (b).

The series capacitance C_s varied from 0.6 to 1.5 pu and load resistance varied between 0.5 to 10 pu. The results show that for source currents smaller or equal to I_n, a capacitor value equal to 1.325 pu will give the highest output power.

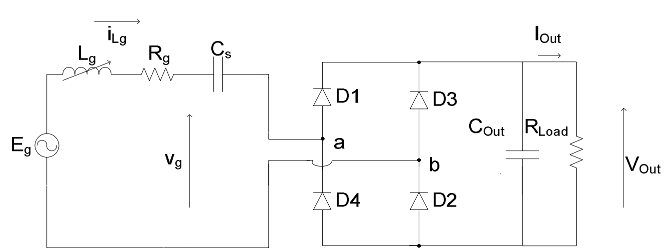

Fig. 8: Series compensated diode-bridge rectifier with constant voltage load.

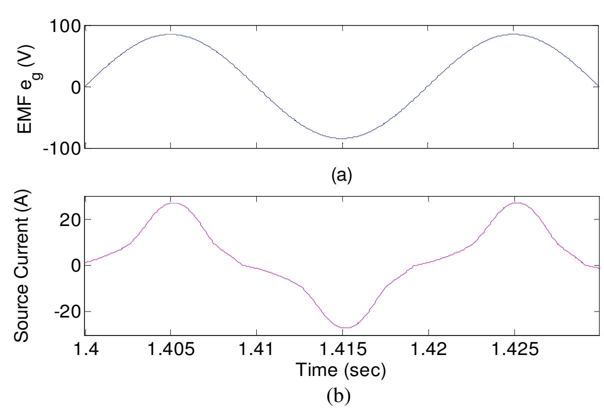

Fig. 9: (a) The source EMF Voltage and (b) source current with C_S=1.32, E_g=1 pu, f=1 pu.

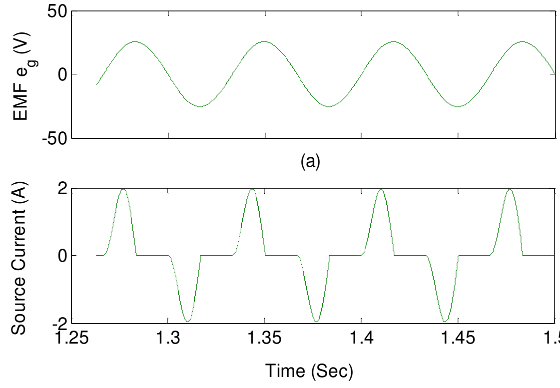

(b)

Fig. 10: (a) The source EMF Voltage (b) source current for the series compensated VSR with saturable inductor, C_S=1.32 pu , E_g=0.3 pu.

DPF (cos(φ)) and distortion factor (DISF) characteristics versus source frequency (EMF voltage) for peak power are shown in figure 11. It is interesting to see that distortion factor will increase below 0.9 pu speed as the effect of saturation decreases, however, it will begin to decrease below 0.6 pu speed as the rectifier enters into the discontinuous conduction mode. Since the optimal capacitor was used to compensate the effective inductance at nominal conditions, the displacement factor (cos(φ)) will be equal to unity. However, as speed decreases, saturation will prove to be an advantage and cos(φ) will not degrade as rapidly as in the case of an unsaturated inductance. This could be explained by the fact that the effective value of the saturable inductance will increase and the larger selected capacitor will become a better choice for the lower frequencies.

The peak extractable power at each frequency (EMF voltage) is presented along with the optimal turbine power curve in figure 12. As could be seen, the series compensation could not deliver the optimal power from the wind turbine below 0.7 pu speed.

III. COMPARISON OF THE SHUNT AND SERIES COMPENSATED VSR CONSIDERING SATURATION

As shown in sections I and II (and as could be seen in figure 13 for the speeds below 0.7 pu), the series compensated rectifier will supply a smaller output power compared to shunt compensated rectifier. Table 2-2 summarizes the operating conditions for both shunt and series compensation circuits with saturable source inductors at their maximum output power (at nominal speed) where η represents the efficiency, $I_{C(rms)}$ is the RMS current in the compensation capacitor, and $V_{C(max)}$ is the peak voltage on the compensation capacitor.

In the case of the shunt capacitor, output voltages are higher and the current in the diode rectifier is lower compared to the series compensation. This could explain the higher efficiency in the former case. For the purpose of efficiency calculation, the capacitor ESR (Equivalent Series Resistance) has been neglected. This means that the efficiency will further deteriorate due to higher capacitor currents in the series compensation if capacitor ESR is taken into consideration.

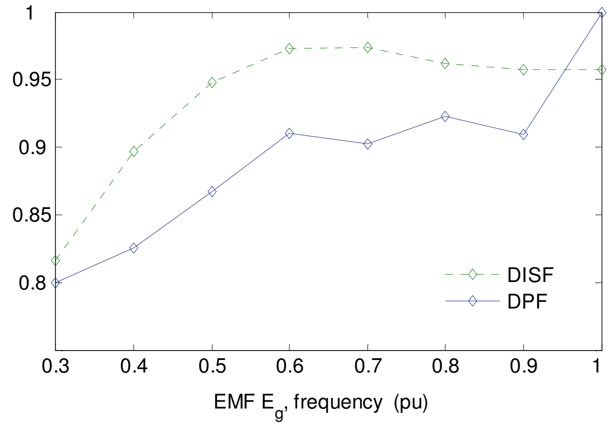

Fig. 11: cos (φ) (DPF) and distortion factor (DISF) characteristics versus source frequency (EMF voltage) for series compensated VSR with saturable source inductance.

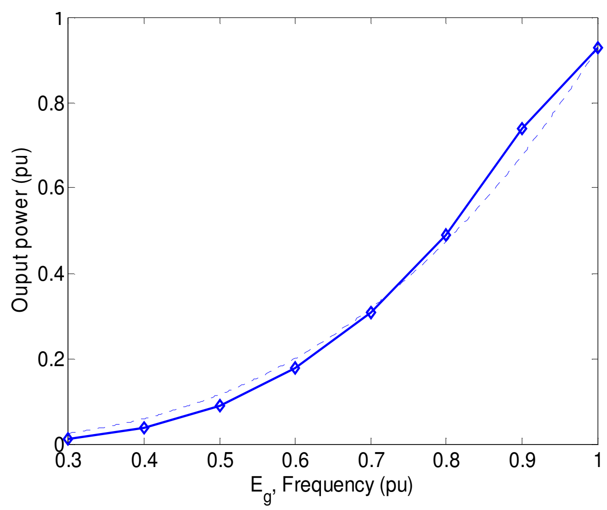

Fig. 12: Maximum extractable output power versus source frequency (line), the optimal turbine power curve (dotted).

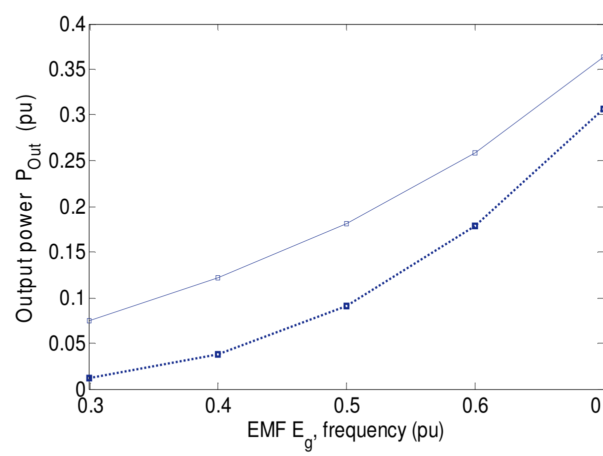

Fig. 13: Maximum extractable output power versus source frequency for shunt compensated VSR (line), for series compensated VSR (dotted).

The size, and as a consequence, the price of a capacitor, are a function of CV. This means that the size of the capacitor needed in series compensation will be approximately 2.2 times greater than shunt compensation.

IV. CONCLUSION

It could be concluded that an uncontrolled rectifier with shunt compensation is an interesting rectifier choice for a TFPM machine in a wind turbine application. Despite saturation, the source current will have low distortion during the whole speed range even at nominal conditions where saturation has a more pronounced effect and high efficiencies could be attained. It was also shown that the series compensated rectifier could not extract the optimal turbine power in the whole speed range.

Though shunt compensation is highly recommended for a wind turbine application for which power requirements are lower at lower speeds, it will not be the proper choice where output power should be proportional to machine speed.

V. REFERENCES

[1] M.R. Dubois, H. Polinder, 'Study of TFPM machines with toothed rotor applied to direct-drive generators for wind turbines'. In *Proceedings of the Nordic workshop on power and industrial electronics (NORPIE),* Trondheim, paper number 71, June 2004, pp. 14-16.

[2] M.R. Dubois, *Optimized permanent magnet generator topologies for direct-drive wind turbines*, Les Imprimeries ABC Inc. Lévis, Canada: 2006, pp. 100.

[3] Tan, K.; Yao, T.T.; Islam, S., "Effect of loss modeling on optimum operation of wind turbine energy conversion systems," The 7th International Power Engineering Conference, 2005, Nov.-Dec. 2005, pp. 92 - 98

Table II: Operating conditions for both shunt and series compensated VSRs with saturable source inductors at their maximum output power

	C_{Sh}, C_S *pu*	C_{Out} *pu*	E_g *pu*	I_{Lg} *pu*	$\frac{I_{L_g,1}}{I_{L_g,nom}}$	*cos* (*φ*)	$\frac{V_{Out}}{E}$	P_{Out} pu	$I_{C(rms)}$ pu	$\frac{V_{C(\max)}}{E}$	η. %
Shunt Cap.	0.625	26	1	1	0.98	1	1.24	0.96	0.67	1.3	98.5
Series Cap.	1.32	26	1	1	0.96	1	0.75	0.93	1	1.35	97.3